

## Article

# Effects of Glutathione-Enriched Inactive Dry Yeast on the Flavor Profile of Kiwi Wine

Zhibo Yang <sup>1,2,†</sup>, Chuan Song <sup>3,†</sup>, Qiuyu Lan <sup>4</sup>, Bin Hu <sup>2</sup>, Zonghua Ao <sup>3</sup>, Suyi Zhang <sup>3</sup>, Junni Tang <sup>1</sup>, Xin Du <sup>5</sup>, Chenglin Zhu <sup>1,\*</sup> and Luca Laghi <sup>4</sup>

<sup>1</sup> College of Pharmacy and Food, Southwest Minzu University, Chengdu 610041, China; yangzhibo@stu.sicau.edu.cn (Z.Y.); junneytang@swun.edu.cn (J.T.)

<sup>2</sup> College of Food Science, Sichuan Agricultural University, Ya'an 625014, China; hubin2555@sina.com

<sup>3</sup> Luzhou Laojiao Co., Ltd., Luzhou 646000, China; songchuan@lzlj.com (C.S.); aozh@lzlj.com (Z.A.); zhangsy@lzlj.com (S.Z.)

<sup>4</sup> Department of Agricultural and Food Sciences, University of Bologna, 47521 Cesena, Italy; lanqiuyu211@gmail.com (Q.L.); l.laghi@unibo.it (L.L.)

<sup>5</sup> College of Chemistry and Life Sciences, Chengdu Normal University, Chengdu 611130, China; 081056@ednu.edu.cn

\* Correspondence: chenglin.zhu@swun.edu.cn; Tel.: +86-028-85928478

† These authors contributed equally to this work.

**Abstract:** This study aimed to explore the influence of glutathione-enriched inactive dry yeast (g-IDY) addition on the changes in aroma and taste compounds in kiwi wine (KW), produced from green-, red-, and yellow-flesh kiwifruits. In total, 42 aroma compounds and 67 taste compounds were characterized using GC-IMS and <sup>1</sup>H-NMR, respectively. Among them, six aroma compounds and thirty-one taste compounds were determined as key compounds based on a *t*-test, variable importance in projection scores, and relative odor activity value. Results indicated that g-IDY addition significantly decreased the concentration of hexyl acetate and increased the concentrations of 1-hexanol-M and pentanal in KW produced from green- and yellow-flesh kiwifruits. Pearson correlation analysis revealed strong associations between key aroma and taste compounds, particularly highlighting significant negative correlations between amino acids and aroma compounds. The findings could shed light on KW processing optimization and provide theoretical support for integrating g-IDY into KW industrial production.

**Keywords:** kiwi wine; glutathione-enriched inactive dry yeast; aroma compounds; taste compounds; multivariate analysis



Academic Editor: Maurizio Ciani

Received: 13 April 2025

Revised: 6 May 2025

Accepted: 12 May 2025

Published: 15 May 2025

**Citation:** Yang, Z.; Song, C.; Lan, Q.; Hu, B.; Ao, Z.; Zhang, S.; Tang, J.; Du, X.; Zhu, C.; Laghi, L. Effects of Glutathione-Enriched Inactive Dry Yeast on the Flavor Profile of Kiwi Wine. *Foods* **2025**, *14*, 1760. <https://doi.org/10.3390/foods14101760>

**Copyright:** © 2025 by the authors. Licensee MDPI, Basel, Switzerland. This article is an open access article distributed under the terms and conditions of the Creative Commons Attribution (CC BY) license (<https://creativecommons.org/licenses/by/4.0/>).

## 1. Introduction

Glutathione (GSH), a tripeptide composed of L-glutamate, L-cysteine, and glycine, offers a protective effect on desirable wine aromas, mitigates the formation of off-flavors, and reduces the formation of browning pigments [1,2]. Considering its beneficial impact on wine quality, the International Organization of Vine and Wine (OIV) has endorsed the treatment of must and wine with GSH [3]. However, the application of GSH in winemaking is constrained by regulatory dosage limits and high production costs. Consequently, there is a pressing necessity to explore and implement viable alternatives to pure GSH in the wine industry.

Inactive dry yeast (IDY) refers to yeast that has undergone thermal inactivation after cultivation under aerobic conditions in sugar-rich media. According to the manufacturing processes, commercially available IDY products can be categorized into four types: inactive

yeast, yeast autolysates, yeast hulls or walls, and yeast extracts [4]. Among these products, glutathione-enriched IDY (g-IDY) is commonly utilized in brewing as a substitute for pure GSH. Research has shown that g-IDY can either release GSH directly into wine and/or provide precursors for GSH synthesis, thereby increasing the GSH content in the wine [5]. Additionally, g-IDY has been observed to release complex nitrogen-containing volatile compounds into wine, influencing its aroma profile [6].

Kiwi wine (KW), a fermented alcoholic beverage produced from kiwifruit through yeast-driven alcoholic fermentation, is nicely tailored for consumers seeking low-alcohol beverages, given its inherently low alcohol content, suggesting substantial market potential for growth [7]. The differences in kiwifruit material come from their variety. Various varieties may exhibit different flesh colors, which can be green, red, or yellow, and there are significant differences in the flavor of KW produced by different kiwifruit varieties [8]. The flavor profile of KW encompasses both its aroma and taste profiles, which are crucial factors influencing consumer preferences [9]. Aroma, primarily shaped by volatile compounds, such as alcohols, aldehydes, esters, acids, and phenols, plays a pivotal role in defining the organoleptic attributes of KW [10]. Additionally, taste compounds, including organic acids and free amino acids, also significantly contribute to the aroma and taste profiles of wines through various chemical, biochemical, and sensory interactions [4]. For instance, during wine fermentation, amino acids could enhance the complexity of flavor by imparting freshness, sweetness, bitterness, and astringency, directly or through conversion into volatile compounds [11].

The relationship between amino acids and volatile components in KW fermented by green-flesh kiwifruit with the addition of g-IDY was investigated in a previous study [4]. Meanwhile, in terms of taste compounds, apart from amino acids, KW contains a large number of organic acids, sugars, and polyphenolic compounds, and the effect of the addition of g-IDY on these substances is unknown. In order to fill such gaps, this study aimed to investigate the effect of g-IDY addition on the aroma and taste profiles dominated by volatile and non-volatile compounds in KW produced from green-, yellow-, and red-flesh kiwifruits. The raw materials were selected from the most representative and currently common kiwifruit varieties with different flesh colors, namely Hayward (green flesh), Donghong (red flesh), and Jinshi (yellow flesh). Several analytical techniques, previously singularly employed, were here combined to capture the comprehensive sensory characteristics and flavor profiles of KW, namely gas chromatography–ion mobility spectrometry (GC-IMS), proton nuclear magnetic resonance spectroscopy ( $^1\text{H-NMR}$ ), and electronic tongue analysis [12,13]. Meanwhile, multivariate analyses, such as principal component analysis (PCA) and partial least squares discriminant analysis (PLS-DA), were combined to discern variations in the aroma, sensory attributes, and taste properties of KW [14]. The findings could shed light on KW processing optimization and provide theoretical support for integrating g-IDY in KW industrial production.

## 2. Materials and Methods

### 2.1. Materials

Fruits from three cultivars, namely Hayward (green flesh), Donghong (red flesh), and Jinshi (yellow flesh), fully ripe and each weighing approximately 100 g, were collected for this study. The initial sugar content of kiwifruit was 10 °Brix, and the juice yield was 75%. These kiwifruits were harvested in September 2023 from a plantation in Pujiang, Sichuan, China, as shown in Figure S1. Following a previous study of ours [15], the yeast strain employed was *S. cerevisiae* strain RW (Angel Yeast Co., Ltd., Yichang, Hubei, China), selected for its well-documented fermentation characteristics for KW fermentation.

## 2.2. KW Samples

All kiwifruits collected for this study were transported to the laboratory right after harvesting. KW production procedures were conducted on a laboratory scale, as illustrated in Figure 1. In the pretreatment phase, the kiwifruits underwent cleaning, peeling, and crushing. Enzymatic digestion was then performed using pectinase (0.02 g/L, 100,000 U/g, SAS SOFRALAB, Magenta, France) for 2 h. The enzyme digestion temperature was controlled at 40 °C by an HH-8 thermostatic water bath (GUOHUA INSTRUMENT MANUFACTURING Co., Ltd., Changzhou, China). Subsequently, potassium metabisulfite (70 mg/L, Shanghai Yuanye Bio-Technology Co., Ltd., Shanghai, China) was added to prevent browning, and sucrose was incorporated to adjust the initial sugar content to 23 °Brix. Finally, activated yeast (0.2 g/L, *Saccharomyces cerevisiae* RW, Angel Yeast Co., Ltd., Yichang, Hubei, China) was introduced. Prior to fermentation, 1 mL of g-IDY (0.25 g/L) was added to each treated sample, while an equal volume of deionized water was added to samples used as controls. The total fermentation volume was 200 mL, and fermentation was conducted at  $25 \pm 1$  °C for 30 days through a DHP-9162D thermostat (Keelrein Instrument Co., Ltd., Shanghai, China). Each group underwent five replicates. After fermentation, the KW samples were filtered through three layers of sterile gauze and stored at  $-80$  °C until further analysis.

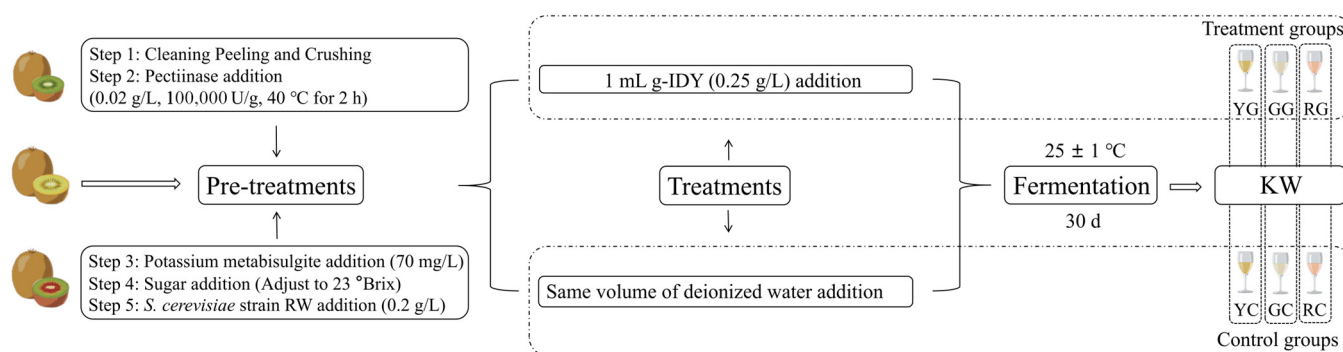


**Figure 1.** KW production workflow.

## 2.3. GC-IMS Analysis

Following Zhang et al. [15], headspace analysis was conducted using a GC-IMS instrument (Flavourspe®, G.A.S. Dortmund Company, Dortmund, Germany), equipped with a syringe and an auto-sampler unit. A Restek MXT-5 column (30 m × 0.53 mm × 1 µm) was employed in GC, with the column and IMS temperatures set at 60 °C and 45 °C, respectively. Samples (1.5 mL) were transferred into a 20 mL headspace glass sampling vial and incubated at 60 °C for 10 min. Subsequently, 200 µL of headspace samples were injected into the injector, operating at 85 °C in splitless mode using a heated syringe. Nitrogen gas (99.999% purity) served as carrier/drift gas, with EPC1 (IMS drift gas) maintained at a flow rate of 150 mL/min. The flow rates were programmed as follows: 2 mL/min for 5 min, 10 mL/min for 10 min, 15 mL/min for 5 min, 50 mL/min for 10 min, and 100 mL/min for 10 min. The qualitative analysis of volatile aroma compounds relied on IMS, supported by the NIST database, integrated within the GC-IMS Library Search. Quantitative analysis was based on peak intensities by means of rectangular integration. The Laboratory Analysis Viewer and Reporter provided by the GC-IMS instrument was utilized to generate fingerprints of each sample.

## 2.4. Relative Odor Activity Value

The relative odor activity value (ROAV) of each flavor compound was calculated according to the methodology described in previous studies [16] and is detailed in the Supporting Material.

### 2.5. $^1\text{H}$ -NMR Analysis

The  $^1\text{H}$ -NMR analysis was performed through a previously established protocol [17]. Solid residues were removed by centrifuging 0.5 mL of each sample at  $18,630\times g$  and  $4^\circ\text{C}$  for 15 min. The resulting supernatant (0.35 mL) was then mixed with bi-distilled water (0.35 mL) and a 200  $\mu\text{L}$  NMR analysis solution ( $\text{D}_2\text{O}$  solution of 3-(trimethylsilyl)-propionic-2,2,3,3- $\text{d}_4$  acid sodium salt (10 mmol/L) + phosphate buffer (1 mol/L) +  $\text{NaN}_3$  (2 mmol/L)), followed by a centrifugation step.

$^1\text{H}$ -NMR spectra of KW samples were recorded using a 600.13 MHz AVANCE III spectrometer (Bruker, Wuhan, China) at 298 K, controlled by Topspin 4.2 software. Experimental conditions are detailed in Figure S2. Following Yang et al. [17], spectral phase adjustment and data processing were performed using the R language. Baseline correction utilized the “rolling ball” algorithm from the R (v.4.4.2) baseline package, and probabilistic quotient normalization (PQN) was applied to normalize molecule concentrations. Compound identification relied on the comparison of peak multiplicity and chemical shifts with standard compound spectra from the Chenomx library (Chenomx Inc., Edmonton, AB, Canada, v.10.1). Signal area was calculated using rectangular integration.

### 2.6. E-Tongue

As detailed in a previous study of ours [18], the analysis of all samples was performed using an  $\alpha$ -Astree E-tongue (Alpha MOS, Toulouse, France). The sensors employed were specifically sensitive to sweetness (ANS), saltiness (CTS), umami (NMS), sourness (AHS), and bitterness (SCS).

In total, 80 mL of a KW sample was transferred into a designated beaker for each E-tongue analysis. Data acquisition time, stirring rate, and analysis duration were set at 120 s, 60 rpm/min, and 3 min, respectively. After each test, the sensors were thoroughly rinsed with deionized water for 30 s. Output values were recorded between 100 and 120 s. Eight test replicates for each sample were conducted, and the mean value of the final five stable measurements was selected for subsequent data analysis.

### 2.7. Statistical Analysis

The R language was utilized to perform a  $t$ -test ( $p < 0.05$ ). Data distribution was normalized using the Box and Cox method [19] prior to conducting univariate analyses. Principal component analysis (PCA) and projections to latent structures–discriminant analysis (PLS-DA) were conducted using MetaboAnalyst 6.0 <https://www.metaboanalyst.ca> (accessed on 20 March 2025). Additionally, the OmicStudio tools <https://www.omicstudio.cn/tool> (accessed on 20 March 2025) were employed for Mantel tests and the construction of correlation networks.

## 3. Results and Discussion

### 3.1. Key Aroma Compounds in KW

Information regarding the identification and analysis of aroma components through GC-IMS is depicted in Figure 2 and Table 1.

As shown in Figure 2a, a total of 42 aroma compounds were characterized by GC-IMS, comprising esters (22), alcohols (7), aldehydes (3), ketones (6), and others (4), as detailed in Table S1. PCA models were developed for each kiwifruit variety in order to assess the influence of the g-IDY addition on the aroma compounds of KW, as shown in Figure 2c,g,k. The first principal component (PC 1) explained 97%, 94.6%, and 94.9% of the overall variance, respectively, thus nicely summarizing the flavor differences between the KW produced with/without g-IDY. PLS-DA models demonstrated strong predictive capability, as can be visually appreciated in Figure 2d,h,l. The VIP scores from PLS-



DA were used to rank the contribution of variables to classification (Figure 2e,i,m). As depicted in Figure 2f, 12 aroma compounds, whose VIP scores are greater than 1, were identified as contributing significantly to classification, as suggested by Wang et al. [20]. The perception of aroma compounds in KW is influenced by both their concentration and threshold. Relative odor activity value (ROAV) analysis was used to identify key aroma compounds by considering their threshold. Ethyl acetate, recognized for its fruity-sweet aroma [21], was selected as a reference due to its high relative content (8.7%) and low threshold (0.005 mg/kg), underscoring its significant impact on KW's overall aroma profile. Compounds with ROAV > 1 are major contributors to flavor, while those with a ROAV between 0.1 and 1 can modify the overall aroma. Table S1 lists 22 aroma compounds with ROAVs exceeding 1, predominantly esters, emphasizing their pivotal roles in shaping KW's aroma characteristics. Figure 2j illustrates six key aroma compounds filtered based on the criteria of ROAV > 1,  $p < 0.05$ , and VIP > 1, namely 1-hexanol-M, ethyl hexanoate, hexyl acetate-D, hexyl acetate-M, isoamyl acetate-D, and pentanal.

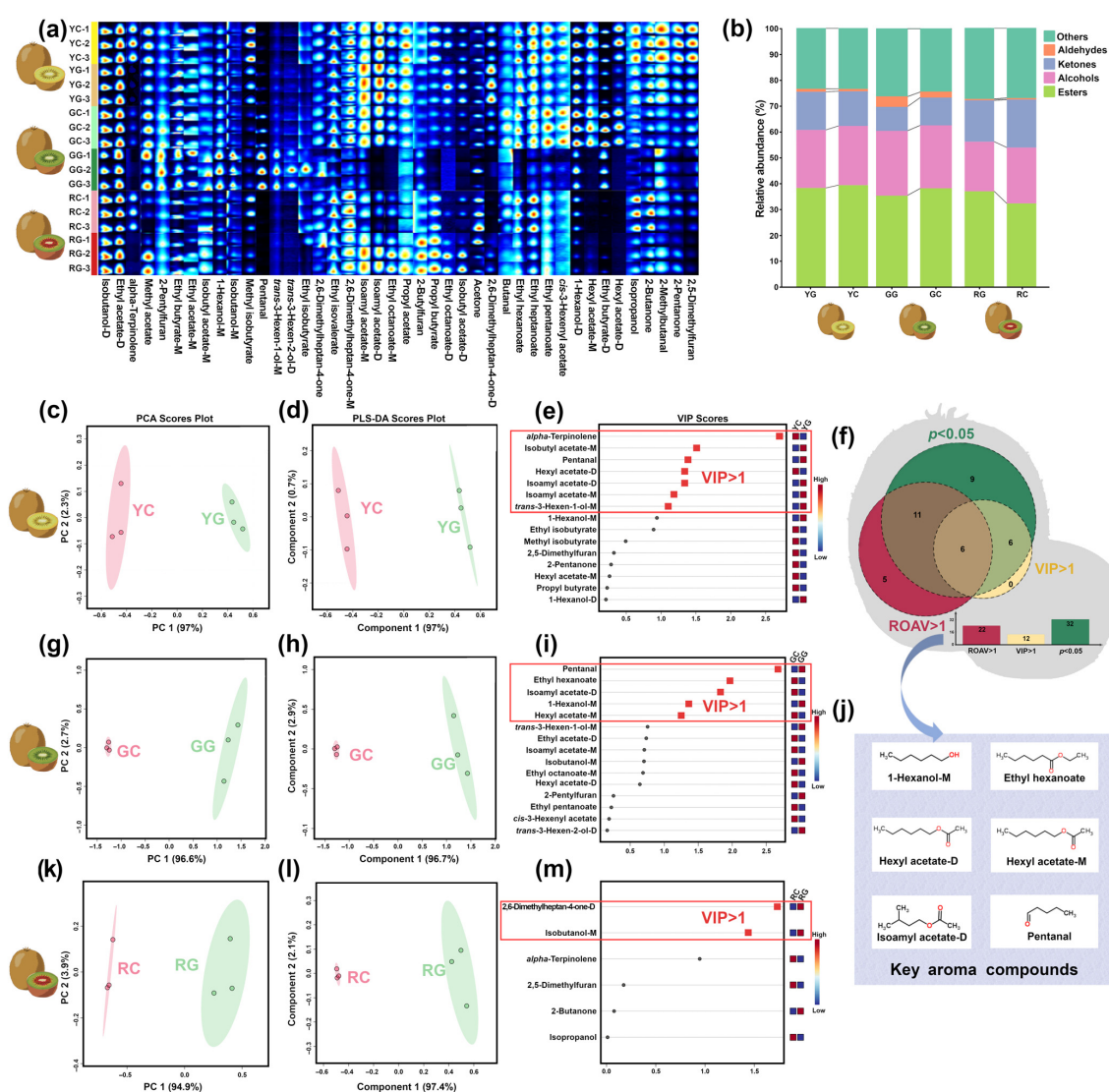


**Figure 2.** Fingerprint plot (a) and bar chart (b) representing the variation in the concentration of molecules in different groups. PCA scores plot (c,g,k), PLS-DA scores plot (d,h,l), and VIP scores (e,i,m) of the aroma compounds in the KW samples. Venn plot of  $p < 0.05$ , ROAV > 1, and VIP > 1 of the aroma compounds in KW produced with/without the addition of g-IDY (f). The key aroma compounds for KW (j).

Table 1. Information about key aroma compounds.

Compounds	CAS	Peak Intensity		<i>p</i> Value	Trend	Peak Intensity		<i>p</i> Value	Trend	Peak Intensity		<i>p</i> Value	Trend	Odor Threshold Value (mg/Kg)	ROAV					
		GG	GC			RG	RC			YG	YC				GG	GC	RG	RC	YG	YC
Ethyl hexanoate	123-66-0	$8.98 \times 10^2 \pm 80.8$	$2.54 \times 10^3 \pm 1.75 \times 10^2$	0.013	↑	$2.81 \times 10^3 \pm 1.26 \times 10^2$	$3.20 \times 10^3 \pm 3.46 \times 10^2$	0.085	=	$2.46 \times 10^3 \pm 92.6$	$1.97 \times 10^3 \pm 29.1$	0.060	=	0.005	9.70	41.40	34.83	49.45	36.49	35.91
Hexyl acetate-D	142-92-7	$1.29 \times 10^2 \pm 9.22$	$7.28 \times 10^2 \pm 25.3$	0.001	↑	$1.13 \times 10^2 \pm 17.5$	$1.07 \times 10^2 \pm 31.2$	0.577	=	$2.63 \times 10^2 \pm 7.65$	$5.85 \times 10^2 \pm 1.16 \times 10^2$	0.005	↑	0.002	3.48	29.75	3.48	4.04	9.75	26.66
Hexyl acetate-M	142-92-7	$2.73 \times 10^2 \pm 1.32 \times 10$	$1.43 \times 10^3 \pm 14.8$	0.001	↑	$2.86 \times 10^2 \pm 31.4$	$1.71 \times 10^2 \pm 16.5$	0.157	↓	$8.53 \times 10^2 \pm 15.5$	$1.11 \times 10^3 \pm 1.15 \times 10^2$	0.007	↑	0.002	7.38	58.24	8.90	6.74	31.67	50.63
Isoamyl acetate-D	123-92-2	$1.32 \times 10^2 \pm 8.26$	$1.95 \times 10^3 \pm 1.15 \times 10^2$	0.001	↑	$2.41 \times 10^3 \pm 6.01 \times 10^2$	$8.43 \times 10^2 \pm 3.59 \times 10^2$	0.152	=	$2.87 \times 10^3 \pm 41.9$	$1.86 \times 10^3 \pm 50.4$	0.010	↓	0.088	0.08	1.80	1.72	0.77	2.42	1.92
1-Hexanol-M	111-27-3	$1.18 \times 10^4 \pm 2.02 \times 10^2$	$5.53 \times 10^3 \pm 4.21 \times 10^2$	0.013	↓	$4.12 \times 10^3 \pm 6.82 \times 10^2$	$4.26 \times 10^3 \pm 5.18 \times 10^2$	0.260	=	$5.28 \times 10^3 \pm 1.53 \times 10^2$	$3.85 \times 10^3 \pm 1.42 \times 10^2$	0.040	↓	0.0056	83.59	80.33	45.19	58.78	69.96	62.44
Pentanal	110-62-3	$7.36 \times 10^3 \pm 6.06 \times 10^2$	$1.56 \times 10^3 \pm 77.3$	0.002	↓	$2.68 \times 10^2 \pm 1.93$	$2.62 \times 10^2 \pm 83.1$	0.924	=	$6.72 \times 10^2 \pm 24.3$	$3.95 \times 10^2 \pm 14.2$	0.023	↓	0.022	18.04	5.79	0.75	0.90	2.26	1.63

Data are displayed as mean ± standard deviation (*n* = 5); “↑” represents significant increase, “↓” represents significant decrease, and “=” represents no significant difference (*p* < 0.05).

Esters are mainly generated through substrate esterification and yeast enzymatic metabolism during fermentation [22]. Four esters were identified as key aroma compounds in KW, including ethyl hexanoate, hexyl acetate-D, hexyl acetate-M, and isoamyl acetate-D. Ethyl hexanoate, partly derived from kiwifruit itself [23], exhibited high ROAV in all samples, ranging from 9.70 to 49.45, contributing floral and fruity notes to KW, in agreement with a previous study [24]. Notably, a significantly higher level was only found in KW produced from Hayward (green flesh) kiwifruit with added g-IDY. Previous studies have demonstrated that KW produced by Hayward kiwifruits have the most pronounced aroma among KW produced with different flesh color kiwifruits, which may explain the phenomenon described above [8,25]. Hexyl acetate is formed through the reaction of ethanol with acetyl CoA, amino acids, carbohydrates, and lipids [26]. Its concentration was significantly lower in KW produced from green- and yellow-flesh kiwifruits with added g-IDY, compared to their control counterparts. Such a phenomenon could be a consequence of the content of ethanol in KW, the immediate precursor substance of hexyl acetate through esterification, whose trends were indeed identical in the above groups. On the other hand, the variation in its levels may also be linked to the presence of GSH derived from the g-IDY addition on the distinctive activities of some enzymes (such as ethanol dehydrogenase), which are involved in esters' synthesis and breakdown. A previous study has confirmed that the g-IDY addition could prevent acetaldehyde from being oxidized to the corresponding carboxylic acid, indirectly inhibiting the esterification of alcohols and acids [3]. Isoamyl acetate, imparting desirable banana and pear aromas to KW, was identified as a key aroma compound of KW in previous research [27]. Its levels were significantly decreased in KW produced by green-flesh kiwifruits with added g-IDY, while the opposite was found in KW from yellow kiwifruits with added g-IDY.

Alcohols, contributing to the harmony of the KW aroma, are synthesized through glycolytic pathways, methyl ketone reduction, and amino acid metabolism [28]. In this study, significantly increased levels of 1-hexanol were found in KW produced from green- and yellow-flesh kiwifruits with added g-IDY, compared to their control counterparts. 1-hexanol, a higher alcohol, could be generated in yeast through glycolysis and the Ehrlich pathway [22]. Higher levels of GSH could be beneficial for higher alcohol formation by yeast metabolism, through the alteration of the redox state of cells. In detail, on one hand, GSH brought on by the g-IDY addition could promote the catabolism of the precursor amino acids, such as leucine [29], to produce higher alcohols. On the other hand, several substances (such as yeast cytosol and bicarb) released by g-IDY, could be used as nitrogen sources to promote the production of amino acids in yeast, and in turn to facilitate the formation of higher alcohols [30,31].

Aldehydes are typically formed by the oxidation of alcohols, serving as essential flavor substances in wines and harmonizing the aroma of the wine, even at low concentrations. The content of pentanal was significantly increased in KW produced from green- and yellow-flesh kiwifruits enriched with g-IDY, compared to their control groups. This could be linked to the oxidation of GSH brought on by the g-IDY addition, which promotes the release of free acetaldehyde [32].

### 3.2. Key Taste Components in KW

A total of 67 taste compounds were characterized by  $^1\text{H}$ -NMR, including alcohols and polyols (5), amino acids, peptides, and analogs (19), carbohydrates and carbohydrate conjugates (5), organic acids and derivatives (22), and others (15), as detailed in Table S2. A typical  $^1\text{H}$ -NMR spectrum of KW is shown in Figure S3.

Similarly to aroma compounds, PCA models were calculated to assess the influence of the g-IDY addition on the taste compounds of KW, as shown in Figure 3a,d,g. For the

three varieties of kiwifruit, the first principal component (PC 1) explained 95.2%, 95.7%, and 95.4% of the overall variance, respectively, thus nicely summarizing the taste differences between the KW produced with/without g-IDY. A total of 31 key taste compounds ( $p < 0.05$  and  $VIP > 1$ ) were identified, as illustrated in Figure 3c,f,i and Table 2.

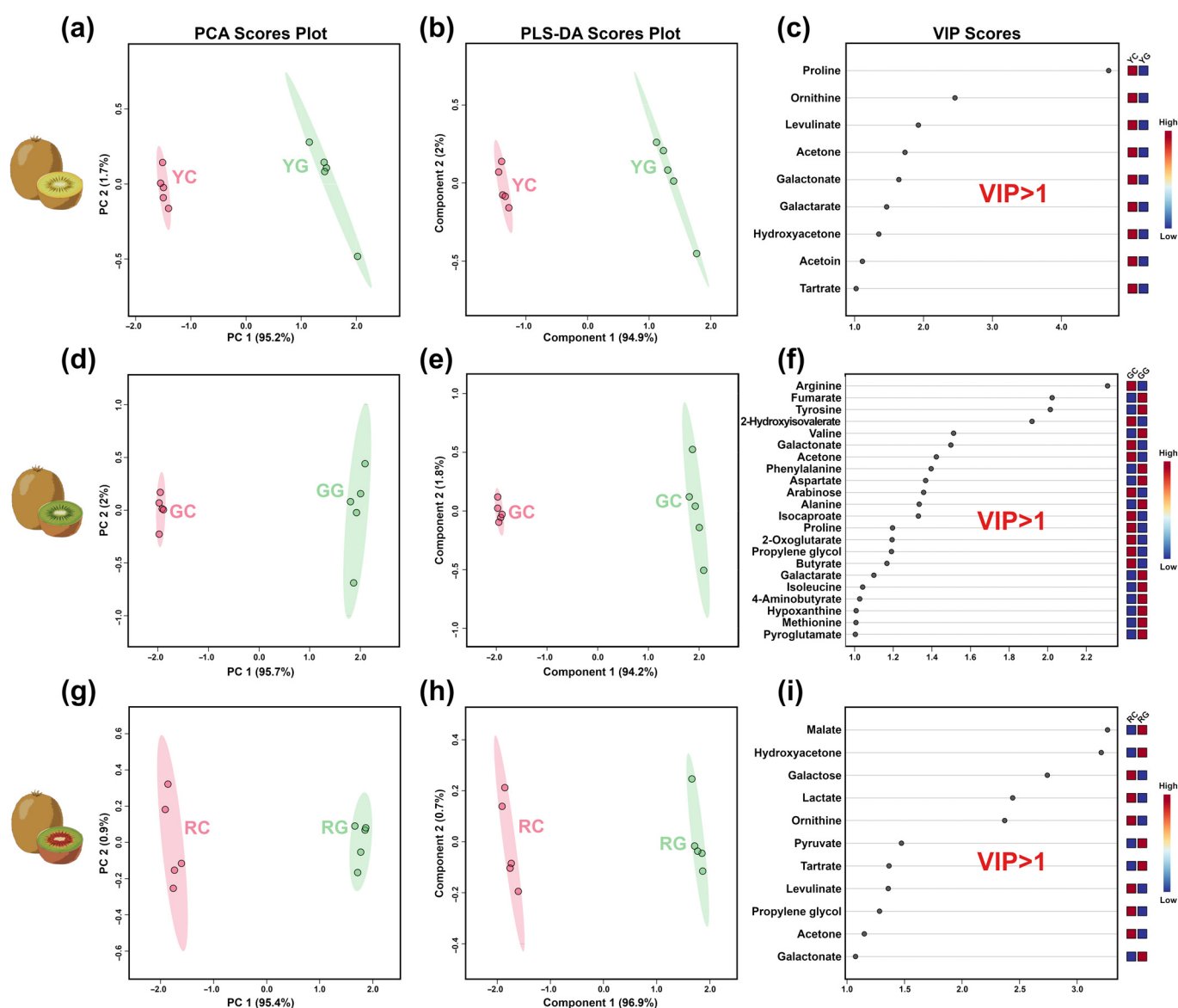


Figure 3. PCA score plots (a,d,g), PLS-DA score plots (b,e,h), and VIP scores (c,f,i) of the taste.



**Table 2.** Information about key taste compounds.

	GC	GG	<i>p</i> Value	Trend	RC	RG	<i>p</i> Value	Trend	YC	YG	<i>p</i> Value	Trend
<b>Alcohols and polyols</b>												
Propylene glycol	$1.47 \times 10^{-3} \pm 6.39 \times 10^{-5}$	$3.75 \times 10^{-4} \pm 1.24 \times 10^{-5}$	<0.01	↓	$4.52 \times 10^{-3} \pm 1.04 \times 10^{-4}$	$1.23 \times 10^{-3} \pm 5.53 \times 10^{-5}$	<0.01	↓	$2.31 \times 10^{-3} \pm 1.29 \times 10^{-4}$	$1.32 \times 10^{-3} \pm 8.65 \times 10^{-5}$	<0.01	↓
<b>Amino acids, peptides, and analogs</b>												
Ornithine	$7.18 \times 10^{-4} \pm 1.46 \times 10^{-4}$	$5.57 \times 10^{-4} \pm 7.69 \times 10^{-5}$	0.073	=	$3.09 \times 10^{-3} \pm 2.69 \times 10^{-4}$	$2.67 \times 10^{-4} \pm 7.71 \times 10^{-5}$	<0.01	↓	$2.14 \times 10^{-4} \pm 6.60 \times 10^{-5}$	$2.75 \times 10^{-5} \pm 1.59 \times 10^{-5}$	<0.01	↓
Alanine	$4.18 \times 10^{-4} \pm 2.09 \times 10^{-5}$	$1.96 \times 10^{-3} \pm 2.33 \times 10^{-5}$	<0.01	↑	$1.04 \times 10^{-3} \pm 9.56 \times 10^{-6}$	$1.43 \times 10^{-3} \pm 9.31 \times 10^{-5}$	<0.01	↑	$8.94 \times 10^{-4} \pm 6.04 \times 10^{-5}$	$1.04 \times 10^{-3} \pm 7.36 \times 10^{-5}$	<0.01	↑
4-Aminobutyrate	$4.24 \times 10^{-4} \pm 4.11 \times 10^{-5}$	$1.39 \times 10^{-3} \pm 1.93 \times 10^{-5}$	<0.01	↑	$1.43 \times 10^{-3} \pm 2.57 \times 10^{-5}$	$1.95 \times 10^{-3} \pm 7.75 \times 10^{-5}$	<0.01	↑	$1.19 \times 10^{-3} \pm 6.13 \times 10^{-5}$	$1.69 \times 10^{-3} \pm 1.27 \times 10^{-4}$	<0.01	↑
Arginine	$2.80 \times 10^{-2} \pm 1.27 \times 10^{-3}$	$1.97 \times 10^{-3} \pm 2.05 \times 10^{-4}$	<0.01	↓	$2.59 \times 10^{-2} \pm 9.24 \times 10^{-4}$	$3.29 \times 10^{-2} \pm 2.23 \times 10^{-3}$	0.115	=	$3.17 \times 10^{-2} \pm 2.27 \times 10^{-3}$	$2.48 \times 10^{-2} \pm 1.42 \times 10^{-3}$	<0.01	↓
Aspartate	$1.13 \times 10^{-4} \pm 2.92 \times 10^{-5}$	$5.38 \times 10^{-4} \pm 5.57 \times 10^{-6}$	<0.01	↑	$1.64 \times 10^{-4} \pm 1.59 \times 10^{-5}$	$1.77 \times 10^{-4} \pm 2.39 \times 10^{-5}$	0.060	=	$1.76 \times 10^{-4} \pm 1.22 \times 10^{-5}$	$2.35 \times 10^{-4} \pm 1.80 \times 10^{-5}$	<0.01	↑
Isoleucine	$3.86 \times 10^{-5} \pm 5.65 \times 10^{-6}$	$1.28 \times 10^{-4} \pm 6.48 \times 10^{-6}$	<0.01	↑	$8.88 \times 10^{-5} \pm 5.62 \times 10^{-6}$	$7.45 \times 10^{-5} \pm 6.19 \times 10^{-6}$	<0.01	↓	$6.83 \times 10^{-5} \pm 7.25 \times 10^{-6}$	$1.03 \times 10^{-4} \pm 9.79 \times 10^{-6}$	<0.01	↑
Methionine	$6.95 \times 10^{-5} \pm 4.79 \times 10^{-6}$	$2.22 \times 10^{-4} \pm 2.50 \times 10^{-6}$	<0.01	↑	$8.52 \times 10^{-5} \pm 5.19 \times 10^{-6}$	$9.31 \times 10^{-5} \pm 5.70 \times 10^{-6}$	0.046	↑	$9.88 \times 10^{-5} \pm 7.84 \times 10^{-6}$	$1.23 \times 10^{-4} \pm 7.70 \times 10^{-6}$	<0.01	↑
Phenylalanine	$8.26 \times 10^{-5} \pm 1.45 \times 10^{-5}$	$4.10 \times 10^{-4} \pm 6.76 \times 10^{-6}$	<0.01	↑	$1.58 \times 10^{-4} \pm 7.19 \times 10^{-6}$	$1.44 \times 10^{-4} \pm 8.66 \times 10^{-6}$	<0.01	↓	$1.24 \times 10^{-4} \pm 1.87 \times 10^{-5}$	$2.35 \times 10^{-4} \pm 1.63 \times 10^{-5}$	<0.01	↑
Proline	$8.09 \times 10^{-5} \pm 6.52 \times 10^{-6}$	$2.16 \times 10^{-5} \pm 8.56 \times 10^{-6}$	<0.01	↓	$5.79 \times 10^{-4} \pm 3.04 \times 10^{-5}$	$1.16 \times 10^{-3} \pm 4.45 \times 10^{-5}$	<0.01	↑	$3.00 \times 10^{-4} \pm 2.42 \times 10^{-5}$	$6.23 \times 10^{-6} \pm 2.72 \times 10^{-6}$	<0.01	↓
Pyroglutamate	$1.20 \times 10^{-4} \pm 2.17 \times 10^{-5}$	$3.90 \times 10^{-4} \pm 9.76 \times 10^{-5}$	<0.01	↑	$5.31 \times 10^{-4} \pm 1.71 \times 10^{-5}$	$5.87 \times 10^{-4} \pm 5.55 \times 10^{-5}$	0.097	=	$2.43 \times 10^{-3} \pm 1.39 \times 10^{-4}$	$2.73 \times 10^{-3} \pm 2.12 \times 10^{-4}$	<0.01	↑
Tyrosine	$4.40 \times 10^{-5} \pm 6.97 \times 10^{-6}$	$4.46 \times 10^{-4} \pm 4.98 \times 10^{-6}$	<0.01	↑	$1.27 \times 10^{-4} \pm 8.64 \times 10^{-6}$	$1.29 \times 10^{-4} \pm 9.17 \times 10^{-6}$	0.010	↑	$8.45 \times 10^{-5} \pm 9.40 \times 10^{-6}$	$1.34 \times 10^{-4} \pm 5.94 \times 10^{-6}$	<0.01	↑
Valine	$4.47 \times 10^{-5} \pm 1.18 \times 10^{-5}$	$2.51 \times 10^{-4} \pm 5.27 \times 10^{-6}$	<0.01	↓	$1.41 \times 10^{-4} \pm 7.09 \times 10^{-6}$	$1.37 \times 10^{-4} \pm 1.55 \times 10^{-5}$	<0.01	↓	$1.13 \times 10^{-4} \pm 1.16 \times 10^{-5}$	$1.45 \times 10^{-4} \pm 1.29 \times 10^{-5}$	<0.01	↑
<b>Carbohydrates and carbohydrate conjugates</b>												
Arabinose	$6.93 \times 10^{-3} \pm 7.90 \times 10^{-4}$	$1.49 \times 10^{-3} \pm 3.60 \times 10^{-4}$	<0.01	↓	$6.91 \times 10^{-3} \pm 6.48 \times 10^{-4}$	$8.89 \times 10^{-3} \pm 7.75 \times 10^{-4}$	0.223	=	$7.28 \times 10^{-3} \pm 5.00 \times 10^{-4}$	$6.99 \times 10^{-3} \pm 1.57 \times 10^{-4}$	0.05	=
Galactose	$5.79 \times 10^{-3} \pm 1.82 \times 10^{-4}$	$6.26 \times 10^{-3} \pm 3.93 \times 10^{-4}$	0.053	=	$4.16 \times 10^{-3} \pm 3.65 \times 10^{-4}$	$2.41 \times 10^{-4} \pm 7.12 \times 10^{-5}$	<0.01	↓	$3.32 \times 10^{-3} \pm 2.99 \times 10^{-4}$	$3.06 \times 10^{-3} \pm 1.76 \times 10^{-4}$	0.631	=
<b>Organic acids and derivatives</b>												
2-Hydroxyisovalerate	$5.29 \times 10^{-5} \pm 8.91 \times 10^{-6}$	$6.28 \times 10^{-6} \pm 2.81 \times 10^{-6}$	<0.01	↓	$5.86 \times 10^{-5} \pm 7.28 \times 10^{-6}$	$5.93 \times 10^{-5} \pm 1.34 \times 10^{-5}$	0.115	=	$1.06 \times 10^{-4} \pm 4.68 \times 10^{-6}$	$7.11 \times 10^{-5} \pm 7.01 \times 10^{-6}$	<0.01	↓
2-Oxoglutarate	$7.92 \times 10^{-4} \pm 5.69 \times 10^{-5}$	$2.02 \times 10^{-4} \pm 2.68 \times 10^{-5}$	<0.01	↓	$2.55 \times 10^{-4} \pm 1.29 \times 10^{-5}$	$6.44 \times 10^{-4} \pm 3.89 \times 10^{-5}$	<0.01	↑	$8.19 \times 10^{-4} \pm 5.95 \times 10^{-5}$	$4.92 \times 10^{-4} \pm 3.13 \times 10^{-5}$	<0.01	↓
Butyrate	$2.91 \times 10^{-4} \pm 2.13 \times 10^{-5}$	$7.62 \times 10^{-5} \pm 1.81 \times 10^{-6}$	<0.01	↓	$1.33 \times 10^{-4} \pm 8.19 \times 10^{-6}$	$2.88 \times 10^{-4} \pm 2.41 \times 10^{-5}$	<0.01	↑	$1.60 \times 10^{-4} \pm 1.13 \times 10^{-5}$	$8.30 \times 10^{-5} \pm 5.85 \times 10^{-6}$	<0.01	↓
Fumarate	$3.92 \times 10^{-5} \pm 5.47 \times 10^{-6}$	$4.03 \times 10^{-4} \pm 5.56 \times 10^{-6}$	<0.01	↑	$3.83 \times 10^{-5} \pm 5.97 \times 10^{-6}$	$5.19 \times 10^{-5} \pm 3.35 \times 10^{-6}$	0.146	=	$4.77 \times 10^{-5} \pm 4.74 \times 10^{-6}$	$7.33 \times 10^{-5} \pm 8.67 \times 10^{-6}$	<0.01	↑
Galactarate	$1.12 \times 10^{-4} \pm 7.06 \times 10^{-6}$	$4.00 \times 10^{-4} \pm 1.30 \times 10^{-5}$	<0.01	↑	$4.81 \times 10^{-5} \pm 3.60 \times 10^{-6}$	$1.09 \times 10^{-4} \pm 6.68 \times 10^{-6}$	<0.01	↑	$1.49 \times 10^{-4} \pm 9.70 \times 10^{-6}$	$3.86 \times 10^{-5} \pm 6.30 \times 10^{-6}$	<0.01	↓

Table 2. Cont.

	GC	GG	<i>p</i> Value	Trend	RC	RG	<i>p</i> Value	Trend	YC	YG	<i>p</i> Value	Trend
Galactonate	$5.13 \times 10^{-4} \pm 7.87 \times 10^{-5}$	$9.49 \times 10^{-5} \pm 2.99 \times 10^{-5}$	<0.01	↓	$3.33 \times 10^{-4} \pm 2.71 \times 10^{-5}$	$1.16 \times 10^{-3} \pm 1.14 \times 10^{-4}$	<0.01	↑	$7.94 \times 10^{-4} \pm 5.10 \times 10^{-5}$	$1.76 \times 10^{-4} \pm 1.01 \times 10^{-5}$	<0.01	↓
Isocaproate	$1.49 \times 10^{-4} \pm 6.91 \times 10^{-6}$	$3.24 \times 10^{-5} \pm 1.79 \times 10^{-6}$	<0.01	↓	$5.62 \times 10^{-5} \pm 4.49 \times 10^{-6}$	$1.34 \times 10^{-4} \pm 1.31 \times 10^{-5}$	<0.01	↑	$7.16 \times 10^{-5} \pm 7.43 \times 10^{-6}$	$3.00 \times 10^{-5} \pm 3.15 \times 10^{-7}$	<0.01	↓
Lactate	$2.26 \times 10^{-3} \pm 1.17 \times 10^{-4}$	$3.95 \times 10^{-3} \pm 2.38 \times 10^{-4}$	<0.01	↑	$2.18 \times 10^{-2} \pm 1.56 \times 10^{-3}$	$1.70 \times 10^{-3} \pm 1.77 \times 10^{-4}$	<0.01	↓	$1.39 \times 10^{-3} \pm 1.18 \times 10^{-4}$	$1.27 \times 10^{-3} \pm 9.28 \times 10^{-5}$	0.320	=
Levulinate	$2.77 \times 10^{-5} \pm 1.80 \times 10^{-6}$	$9.28 \times 10^{-6} \pm 1.46 \times 10^{-6}$	<0.01	↓	$2.71 \times 10^{-5} \pm 1.05 \times 10^{-6}$	$6.85 \times 10^{-6} \pm 8.91 \times 10^{-7}$	<0.01	↓	$3.58 \times 10^{-5} \pm 2.60 \times 10^{-6}$	$6.43 \times 10^{-6} \pm 1.65 \times 10^{-6}$	<0.01	↓
Malate	$3.77 \times 10^{-2} \pm 9.64 \times 10^{-3}$	$3.82 \times 10^{-2} \pm 2.63 \times 10^{-4}$	0.428	=	$6.06 \times 10^{-4} \pm 2.05 \times 10^{-4}$	$2.18 \times 10^{-2} \pm 1.79 \times 10^{-3}$	<0.01	↑	$2.97 \times 10^{-2} \pm 1.84 \times 10^{-3}$	$2.41 \times 10^{-2} \pm 2.06 \times 10^{-3}$	<0.01	↓
Pyruvate	$7.72 \times 10^{-4} \pm 1.15 \times 10^{-4}$	$8.81 \times 10^{-4} \pm 4.93 \times 10^{-5}$	0.103	=	$2.95 \times 10^{-4} \pm 1.24 \times 10^{-5}$	$1.59 \times 10^{-3} \pm 1.75 \times 10^{-4}$	<0.01	↑	$1.26 \times 10^{-3} \pm 1.82 \times 10^{-4}$	$1.82 \times 10^{-3} \pm 3.21 \times 10^{-4}$	<0.01	↑
Tartrate	$7.73 \times 10^{-6} \pm 1.89 \times 10^{-6}$	$3.91 \times 10^{-6} \pm 4.84 \times 10^{-7}$	0.008	↓	$9.08 \times 10^{-6} \pm 1.53 \times 10^{-6}$	$4.33 \times 10^{-5} \pm 6.21 \times 10^{-6}$	<0.01	↑	$1.67 \times 10^{-5} \pm 1.59 \times 10^{-6}$	$6.17 \times 10^{-6} \pm 4.86 \times 10^{-7}$	<0.01	↓
Others												
Acetoin	$1.63 \times 10^{-4} \pm 9.18 \times 10^{-6}$	$8.63 \times 10^{-5} \pm 6.64 \times 10^{-6}$	<0.01	↓	$8.74 \times 10^{-5} \pm 1.03 \times 10^{-5}$	$4.58 \times 10^{-5} \pm 6.11 \times 10^{-6}$	<0.01	↓	$2.65 \times 10^{-4} \pm 1.87 \times 10^{-5}$	$9.12 \times 10^{-5} \pm 8.76 \times 10^{-6}$	<0.01	↓
Acetone	$4.28 \times 10^{-4} \pm 3.83 \times 10^{-5}$	$8.31 \times 10^{-5} \pm 2.87 \times 10^{-6}$	<0.01	↓	$2.87 \times 10^{-4} \pm 1.58 \times 10^{-5}$	$9.05 \times 10^{-5} \pm 7.00 \times 10^{-6}$	<0.01	↓	$4.33 \times 10^{-4} \pm 3.54 \times 10^{-5}$	$8.97 \times 10^{-5} \pm 9.50 \times 10^{-6}$	<0.01	↓
Hydroxyacetone	$2.68 \times 10^{-5} \pm 3.71 \times 10^{-6}$	$2.14 \times 10^{-5} \pm 5.89 \times 10^{-6}$	0.121	↓	$5.27 \times 10^{-6} \pm 2.29 \times 10^{-6}$	$1.71 \times 10^{-4} \pm 2.61 \times 10^{-5}$	<0.01	↑	$6.68 \times 10^{-5} \pm 3.95 \times 10^{-6}$	$1.90 \times 10^{-5} \pm 2.12 \times 10^{-6}$	<0.01	↓
Hypoxanthine	$3.01 \times 10^{-5} \pm 8.31 \times 10^{-6}$	$1.02 \times 10^{-4} \pm 3.76 \times 10^{-5}$	0.011	↑	$2.15 \times 10^{-5} \pm 5.28 \times 10^{-6}$	$2.21 \times 10^{-5} \pm 5.27 \times 10^{-6}$	0.291	=	$4.29 \times 10^{-5} \pm 5.93 \times 10^{-6}$	$3.38 \times 10^{-5} \pm 1.19 \times 10^{-5}$	0.572	=

Data are displayed as mean ± standard deviation (n = 5); “↑” represents significant increase, “↓” represents significant decrease, and “=” represents no significant difference (*p* < 0.05).

Amino acids contribute considerably to the taste profile of KW and serve as precursors for some aroma compounds. Among the key taste compounds, eleven amino acids were identified, underscoring their critical role in determining KW's taste profile. The concentrations of aspartate, isoleucine, phenylalanine, and valine were significantly higher in KW produced from green- and yellow-flesh kiwifruits with added g-IDY, compared to their controls. A parallel, opposite trend was found for proline and arginine. Both isoleucine and valine are crucial precursors for several aroma compound (such as isoamyl acetate and isobutyl acetate) formations by yeast during alcoholic fermentation via the Ehrlich pathway [33]. In our study, trends similar to those of isoamyl acetate and isobutyl acetate were found for valine and isoleucine in KW with added g-IDY, reinforcing the idea that the addition of g-IDY could impact the Ehrlich pathway in yeast.

Organic acids play pivotal roles in the taste profile of KW, imparting pleasant and refreshing sensorial attributes to it [34]. Among the key taste organic acids and derivatives identified in this study, the levels of fumarate, galactarate, and lactate were significantly increased in KW produced from green- and yellow-flesh kiwifruits with added g-IDY, while the levels of malate, 2-hydroxyisovalerate, 2-oxoglutarate, butyrate, and galactonate were significantly decreased. Previous studies have confirmed that lactate, produced by the conversion of malate during malolactic fermentation (MLF), could positively affect the taste profile of wine by adding complexity and balance to the mouthfeel [35]. In our study, the opposite trends observed for lactate and malate in KW were likely due to the beneficial effects of GSH produced by g-IDY on malate conversion during MLF, as reported by Torrea et al. [36].

### 3.3. E-Tongue Analysis

The E-tongue simulates human taste perception by detecting taste characteristics through electronic sensors, enabling an objective assessment of the taste profiles of samples [37]. As illustrated in Figure 4, the main driver of the distribution of KW samples along PC 1 is the varietal differences in kiwifruit, with KW produced by green- and yellow-flesh kiwifruits exhibiting positive PC 1 scores and KW produced by red-flesh kiwifruits exhibiting negative PC 1 scores. PC 2 mainly catches the differences associated with the addition of g-IDY, with KW produced with the addition of g-IDY appearing at positive PC 2 scores and KW without the addition appearing at negative PC 2 scores.

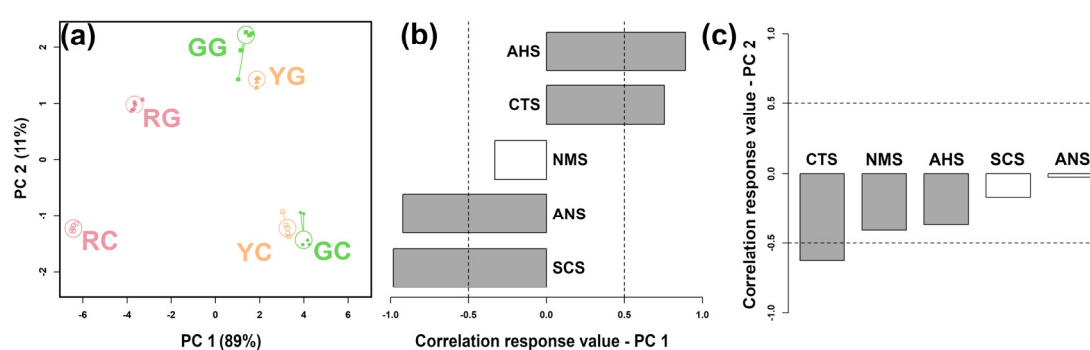


**Figure 4.** An rPCA model set up based on the response values of the E-tongue sensors representing the Scoreplot (a) and Loading plot (b,c). Gray bars (b) display significant correlations between the concentration of each molecule and its importance over the PC.

### 3.4. Correlation Between E-Tongue and Key Taste Compounds

A negative and positive correlation between key taste compounds is indicated, respectively, by blue and red colors in the upper triangular heat map. The color and type of lines indicate the  $r$  and  $p$  values of the Mantel correlations between molecule levels and E-tongue sensor responses, respectively.

To explore the relationship between specific compounds and taste attributes, as well as correlations among taste compounds, a correlation analysis was conducted using E-tongue response values and key taste compounds characterized by  $^1\text{H-NMR}$ , as depicted in Figure 5. Aspartate, which is derived from the degradation of nucleic acids, is associated with both a fresh and savory taste [38]. In our study, aspartate exhibited a significant positive correlation with the CTS sensor, which is sensitive to saltiness, highlighting the contribution of aspartate to the overall taste profile of KW. Proline is a sweet amino acid that exhibits a significant positive correlation with ANS sensors, sensitive to sweetness. Furthermore, lactate, levulinate, malate, and pyruvate demonstrated significant positive correlations with the AHS sensor, which is highly sensitive to sourness, underscoring the critical role of organic acids in the acidity and overall sensory attributes of KW.

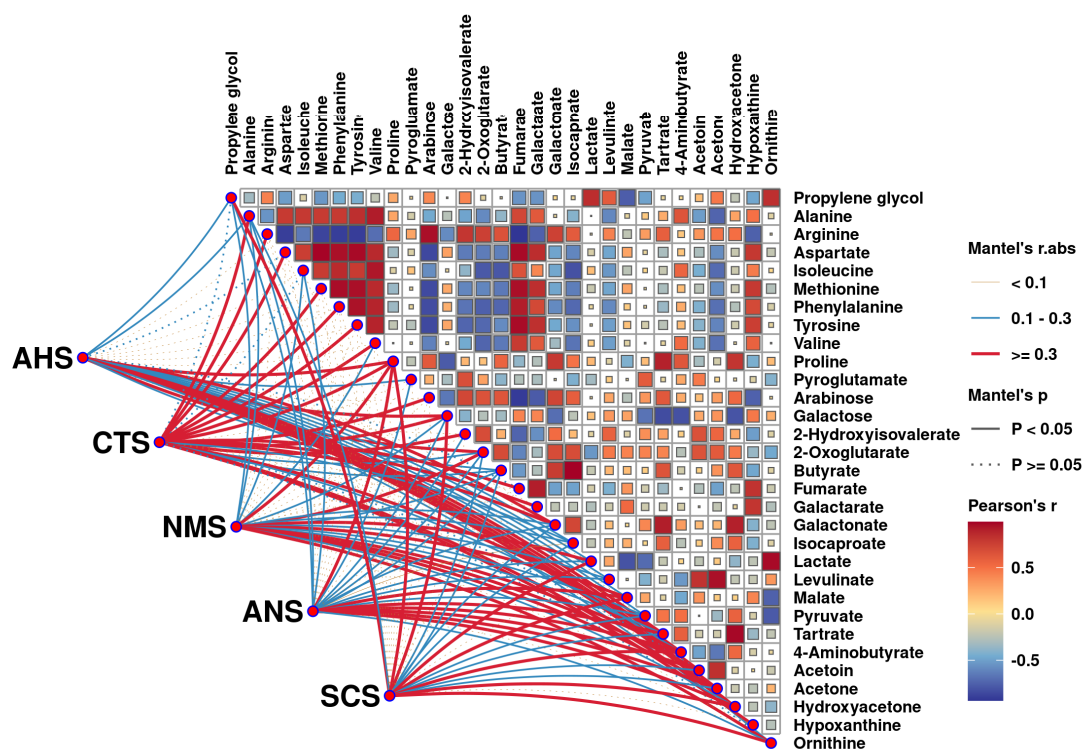


**Figure 5.** Correlations between key taste compounds quantified by  $^1\text{H-NMR}$  and E-tongue sensor responses. A negative and positive correlation between key taste compounds is indicated, respectively, by blue and red colors in the upper triangular heat map. The color and type of lines indicate the  $r$  and  $p$  values of Mantel correlations between molecule levels and E-tongue sensor responses, respectively.

### 3.5. Correlation Between Key Aroma and Taste Compounds

Relationships between key aroma and taste compounds in KW were analyzed based on the Pearson correlation coefficients, as shown in Figure 6. These key aroma and taste compounds significantly influence the aroma and flavor profile in KW, thereby affecting its overall quality [39].

Valine showed a negative correlation with hexyl acetate and ethyl hexanoate. Similarly, isoleucine exhibited negative correlations with ethyl hexanoate, hexyl acetate-D, and hexyl acetate-M. These branched-chain amino acids undergo transamination and oxidative decarboxylation reactions during metabolism, potentially influencing the production of butyrate [40]. Moreover, a negative correlation between 1-hexanol-M and proline was found, probably because amino acids could lead to the formation of higher alcohols via the Ehrlich pathway [41].

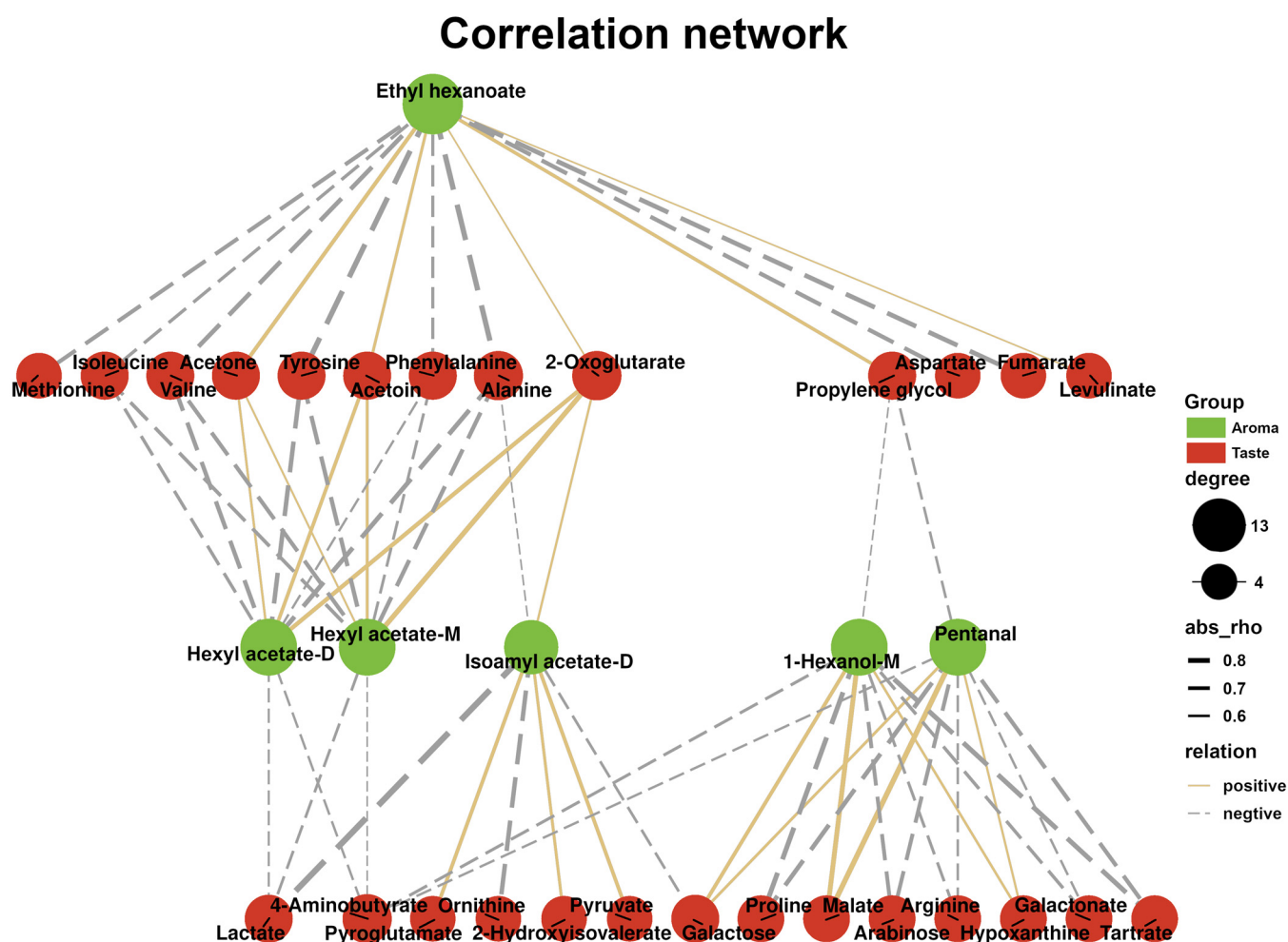


**Figure 6.** Pearson correlation network between key aroma and key taste compounds in KW. Solid yellow lines represent significant positive correlations, and dashed gray lines represent significant negative correlations ( $|r| > 0.5$ ). The thicker the line, the stronger the correlation.

## 4. Conclusions

This study investigated the effects of the g-IDY addition on the flavor profiles of KW from different kiwifruit cultivars, considering both aroma and taste compounds. E-tongue analysis effectively differentiated the taste characteristics of KW fermented with/without the g-IDY addition. The results indicated that the addition of g-IDY had a negative impact on ester production, while positively influencing the production of many amino acids and organic acids. In detail, the levels of fumarate, galactarate, and lactate were significantly increased in KW produced from green- and yellow-flesh kiwifruits with added g-IDY, while the levels of malate, 2-hydroxyisovalerate, 2-oxoglutarate, butyrate, and galactonate were significantly decreased. It is worth noticing that the flavor of KW fermented by green- and yellow-flesh kiwifruits could be more easily altered by the g-IDY addition, compared to those fermented from red-flesh kiwifruit. This study provides supportive data on the effect of g-IDY on the flavor quality of KW made from kiwifruits with different flesh colors and sheds light on the application of the g-IDY addition in the KW industry. Further investigation is required to explore the impact of different levels of the g-IDY addition on the flavor characteristics of KW, in particular for different flesh colors.



**Supplementary Materials:** The following supporting information can be downloaded at: <https://www.mdpi.com/article/10.3390/foods14101760/s1>, Figure S1: Photos of the three kiwis used; Figure S2: The main setting conditions for  $^1\text{H-NMR}$ ; Figure S3:  $^1\text{H-NMR}$  spectrum from one KW sample representative of all the registered spectra. The name of each molecule appears over the signal used for its quantification. To ease the reader's visual inspection, for each portion, a spectrum with a convenient signal-to-noise ratio has been selected; Figures S4–S16: Pictorial description of the molecules' assignment and quantification procedure by Chenomx software (v.10.1). Upper panel—portions of the spectra in white-washed mode. Lower panel—One representative registered spectrum (black line) superimposed to the signals simulated by Chenomx software (red line) for each of the molecules listed. The black and red dashed lines evidence the signals used for quantification purposes; Table S1: Information of all aroma compounds identified by GC-IMS; Table S2: Information of all taste compounds identified by  $^1\text{H-NMR}$ .

**Author Contributions:** Conceptualization, C.Z.; methodology, C.Z. and L.L.; formal analysis, Z.Y. and C.S.; data curation, C.Z. and B.H.; writing—original draft preparation, Z.Y., Q.L., C.Z. and L.L.; writing—review and editing, Z.Y., C.S., Q.L., B.H., Z.A., S.Z., J.T., X.D., C.Z. and L.L.; funding acquisition, C.Z. All authors have read and agreed to the published version of the manuscript.

**Funding:** This work was funded by the Natural Science Foundation of Sichuan Province (Grant No. 2024NSFSC0364), the Fundamental Research Funds for the Central Universities Southwest Minzu University (ZYN2025083), and the Luzhou Laojiao Postdoctoral Research Program.

**Institutional Review Board Statement:** Not applicable.

**Informed Consent Statement:** Not applicable.

**Data Availability Statement:** The original contributions presented in this study are included in the article/Supplementary Materials. Further inquiries can be directed to the corresponding author.

**Conflicts of Interest:** Authors Chuan Song, Zonghua Ao and Suyi Zhang were employed by the company Luzhou Laojiao Co., Ltd. They participated in formal analysis and review the manuscript in the study. The role of the company was GC-IMS analysis. The remaining authors declare that the research was conducted in the absence of any commercial or financial relationships that could be construed as a potential conflict of interest.

## References

1. Sonni, F.; Clark, A.C.; Prenzler, P.D.; Riponi, C.; Scollary, G.R. Antioxidant Action of Glutathione and the Ascorbic Acid/Glutathione Pair in a Model White Wine. *J. Agric. Food Chem.* **2011**, *59*, 3940–3949. [\[CrossRef\]](#) [\[PubMed\]](#)
2. Tomašević, M.; Gracin, L.; Ćurko, N.; Ganić, K.K. Impact of Pre-Fermentative Maceration and Yeast Strain Along with Glutathione and  $\text{SO}_2$  Additions on the Aroma of *Vitis vinifera* L. Pošip Wine and Its Evaluation During Bottle Aging. *LWT* **2017**, *81*, 67–76. [\[CrossRef\]](#)
3. Xu, J.; Qi, Y.; Zhang, J.; Liu, M.; Wei, X.; Fan, M. Effect of Reduced Glutathione on the Quality Characteristics of Apple Wine During Alcoholic Fermentation. *Food Chem.* **2019**, *300*, 125130. [\[CrossRef\]](#) [\[PubMed\]](#)
4. Liu, D.; Qi, Y.; Zhao, N.; Cao, Y.; Xu, J.; Fan, M. Multivariate Analysis Reveals Effect of Glutathione-Enriched Inactive Dry Yeast on Amino Acids and Volatile Components of Kiwi Wine. *Food Chem.* **2020**, *329*, 127086. [\[CrossRef\]](#) [\[PubMed\]](#)
5. Kritzinger, E.C.; Stander, M.A.; Du Toit, W.J. Assessment of Glutathione Levels in Model Solution and Grape Ferments Supplemented with Glutathione-Enriched Inactive Dry Yeast Preparations Using a Novel UPLC-MS/MS Method. *Food Addit. Contam. Part A* **2013**, *30*, 80–92. [\[CrossRef\]](#)
6. Xie, L.; Yu, K.; Xiao, X.; Wei, Z.; Xiong, R.; Du, Y.; Li, Y.; Ma, Y. Study on the Kinetic Model of Mixed Fermentation by Adding Glutathione-Enriched Inactive Dry Yeast. *Fermentation* **2024**, *10*, 329. [\[CrossRef\]](#)
7. Li, S.; Bi, P.; Sun, N.; Gao, Z.; Chen, X.; Guo, J. Characterization of Different Non-Saccharomyces Yeasts via Mono-Fermentation to Produce Polyphenol-Enriched and Fragrant Kiwi Wine. *Food Microbiol.* **2022**, *103*, 103867. [\[CrossRef\]](#)
8. Zhang, Q.; Ma, Y.; Wan, F.; Cai, Z.; Zeng, R.; Tang, J.; Nie, X.; Jiang, X.; Zhu, C.; Laghi, L. Comprehensive Comparison of Flavor and Metabolomic Profiles in Kiwi Wine Fermented by Kiwifruit Flesh with Different Colors. *LWT* **2024**, *208*, 116719. [\[CrossRef\]](#)
9. Li, N.; Wang, Q.-Q.; Xu, Y.-H.; Li, A.-H.; Tao, Y.-S. Increased Glycosidase Activities Improved the Production of Wine Varietal Odorants in Mixed Fermentation of *P. fermentans* and High Antagonistic *S. cerevisiae*. *Food Chem.* **2020**, *332*, 127426. [\[CrossRef\]](#)

10. Ling, M.; Bai, X.; Cui, D.; Shi, Y.; Duan, C.; Lan, Y. An Efficient Methodology for Modeling to Predict Wine Aroma Expression Based on Quantitative Data of Volatile Compounds: A Case Study of Oak Barrel-Aged Red Wines. *Food Res. Int.* **2023**, *164*, 112440. [[CrossRef](#)]
11. Delompré, T.; Guichard, E.; Briand, L.; Salles, C. Taste Perception of Nutrients Found in Nutritional Supplements: A Review. *Nutrients* **2019**, *11*, 2050. [[CrossRef](#)] [[PubMed](#)]
12. Liu, C.; Li, M.; Ren, T.; Wang, J.; Niu, C.; Zheng, F.; Li, Q. Effect of *Saccharomyces Cerevisiae* and Non-*Saccharomyces* Strains on Alcoholic Fermentation Behavior and Aroma Profile of Yellow-Fleshed Peach Wine. *LWT* **2022**, *155*, 112993. [[CrossRef](#)]
13. Zhu, C.; Yang, Z.; Lu, X.; Yi, Y.; Tian, Q.; Deng, J.; Jiang, D.; Tang, J.; Laghi, L. Effects of *Saccharomyces Cerevisiae* Strains on the Metabolomic Profiles of Guangan Honey Pear Cider. *LWT* **2023**, *182*, 114816. [[CrossRef](#)]
14. Yang, Y.; Ai, L.; Mu, Z.; Liu, H.; Yan, X.; Ni, L.; Zhang, H.; Xia, Y. Flavor Compounds with High Odor Activity Values (OAV > 1) Dominate the Aroma of Aged Chinese Rice Wine (Huangjiu) by Molecular Association. *Food Chem.* **2022**, *383*, 132370. [[CrossRef](#)] [[PubMed](#)]
15. Zhang, Q.; Ma, J.; Yang, Y.; Deng, J.; Zhu, K.; Yi, Y.; Tang, J.; Jiang, X.; Zhu, C.; Laghi, L. Effects of *S. cerevisiae* Strains on the Sensory Characteristics and Flavor Profile of Kiwi Wine Based on E-Tongue, GC-IMS and <sup>1</sup>H-NMR. *LWT* **2023**, *185*, 115193. [[CrossRef](#)]
16. Zhou, B.; Liu, X.; Lan, Q.; Wan, F.; Yang, Z.; Nie, X.; Cai, Z.; Hu, B.; Tang, J.; Zhu, C.; et al. Comparison of Aroma and Taste Profiles of Kiwi Wine Fermented with/without Peel by Combining Intelligent Sensory, Gas Chromatography-Mass Spectrometry, and Proton Nuclear Magnetic Resonance. *Foods* **2024**, *13*, 1729. [[CrossRef](#)]
17. Yang, Z.; Lan, Q.; Liu, X.; Cai, Z.; Zeng, R.; Tang, J.; Jiang, X.; Zhu, C.; Hu, B.; Laghi, L. Effects of Pretreatment Methods on the Flavor Profile and Sensory Characteristics of Kiwi Wine Based on <sup>1</sup>H NMR, GC-IMS and E-tongue. *LWT* **2024**, *203*, 116375. [[CrossRef](#)]
18. Zhao, X.; Feng, J.; Laghi, L.; Deng, J.; Dao, X.; Tang, J.; Ji, L.; Zhu, C.; Picone, G. Characterization of Flavor Profile of “Nanx Wudl” Sour Meat Fermented from Goose and Pork Using Gas Chromatography–Ion Mobility Spectrometry (GC–IMS) Combined with Electronic Nose and Tongue. *Foods* **2023**, *12*, 2194. [[CrossRef](#)]
19. Box, G.E.P.; Cox, D.R. An Analysis of Transformations. *J. R. Stat. Soc. Ser. B Stat. Methodol.* **1964**, *26*, 211–243. [[CrossRef](#)]
20. Wang, S.; Zhang, Q.; Zhao, P.; Ma, Z.; Zhang, J.; Ma, W.; Wang, X. Investigating the Effect of Three Phenolic Fractions on the Volatility of Floral, Fruity, and Aged Aromas by HS-SPME-GC-MS and NMR in Model Wine. *Food Chem. X* **2022**, *13*, 100281. [[CrossRef](#)]
21. Zang, X.; Du, Q.; Qu, R.; Ye, D.; Lu, Y.; Liu, Y. Analysis of Volatile Aroma Compounds and Sensory Characteristics Contributing to Regional Style of Red Wines from Hexi Corridor Based on Sixteen Grape Varieties/Clones. *Fermentation* **2022**, *8*, 501. [[CrossRef](#)]
22. Liu, B.; Yang, Y.; Ren, L.; Su, Z.; Bian, X.; Fan, J.; Wang, Y.; Han, B.; Zhang, N. HS-GC-IMS and PCA to Characterize the Volatile Flavor Compounds in Three Sweet Cherry Cultivars and Their Wines in China. *Molecules* **2022**, *27*, 9056. [[CrossRef](#)]
23. Zhang, Q.-A.; Zheng, H.; Lin, J.; Nie, G.; Fan, X.; García-Martín, J.F. The State-of-the-Art Research of the Application of Ultrasound to Winemaking: A Critical Review. *Ultrason. Sonochem.* **2023**, *95*, 106384. [[CrossRef](#)] [[PubMed](#)]
24. Lan, T.; Wang, J.; Yuan, Q.; Lei, Y.; Peng, W.; Zhang, M.; Li, X.; Sun, X.; Ma, T. Evaluation of the Color and Aroma Characteristics of Commercially Available Chinese Kiwi Wines via Intelligent Sensory Technologies and Gas Chromatography-Mass Spectrometry. *Food Chem. X* **2022**, *15*, 100427. [[CrossRef](#)]
25. Zhou, Y.; Fei, G.; Hasan, K.M.F.; Kang, Y.; Wu, Y.; Li, H.; Zhou, S. Cultivar Difference Characterization of Kiwifruit Wines on Phenolic Profiles, Volatiles and Antioxidant Activity. *Food Chem. X* **2023**, *18*, 100691. [[CrossRef](#)]
26. Russo, P.; Tufariello, M.; Renna, R.; Tristezza, M.; Taurino, M.; Palombi, L.; Capozzi, V.; Rizzello, C.G.; Grieco, F. New Insights into the Oenological Significance of *Candida zemplinina*: Impact of Selected Autochthonous Strains on the Volatile Profile of Apulian Wines. *Microorganisms* **2020**, *8*, 628. [[CrossRef](#)] [[PubMed](#)]
27. Lu, Y.; Liu, Y.; Lv, J.; Ma, Y.; Guan, X. Changes in the Physicochemical Components, Polyphenol Profile, and Flavor of Persimmon Wine During Spontaneous and Inoculated Fermentation. *Food Sci. Nutr.* **2020**, *8*, 2728–2738. [[CrossRef](#)]
28. Chen, M.; Chen, X.; Guo, Y.; Liu, N.; Wang, K.; Gong, P.; Zhao, Y.; Cai, L. Effect of In Vitro Digestion and Fermentation of Kiwifruit Pomace Polysaccharides on Structural Characteristics and Human Gut Microbiota. *Int. J. Biol. Macromol.* **2023**, *253*, 127141. [[CrossRef](#)]
29. Liu, M.; Yang, K.; Qi, Y.; Zhang, J.; Fan, M.; Wei, X. Fermentation Temperature and the Phenolic and Aroma Profile of Persimmon Wine. *J. Inst. Brew.* **2018**, *124*, 269–275. [[CrossRef](#)]
30. Šuklje, K.; Antalick, G.; Buica, A.; Coetzee, Z.A.; Brand, J.; Schmidtke, L.M.; Vivier, M.A. Inactive Dry Yeast Application on Grapes Modify Sauvignon Blanc Wine Aroma. *Food Chem.* **2016**, *197*, 1073–1084. [[CrossRef](#)]
31. Valero, E.; Millán, C.; Ortega, J.M.; Mauricio, J.C. Concentration of Amino Acids in Wine After the End of Fermentation by *Saccharomyces cerevisiae* Strains. *J. Sci. Food Agric.* **2003**, *83*, 830–835. [[CrossRef](#)]
32. Bueno, M.; Carrascón, V.; Ferreira, V. Release and Formation of Oxidation-Related Aldehydes during Wine Oxidation. *J. Agric. Food Chem.* **2016**, *64*, 608–617. [[CrossRef](#)]

33. Procopio, S.; Krause, D.; Hofmann, T.; Becker, T. Significant Amino Acids in Aroma Compound Profiling During Yeast Fermentation Analyzed by PLS Regression. *LWT Food Sci. Technol.* **2013**, *51*, 423–432. [[CrossRef](#)]
34. Huang, J.; Wang, Y.; Ren, Y.; Wang, X.; Li, H.; Liu, Z.; Yue, T.; Gao, Z. Effect of Inoculation Method on the Quality and Nutritional Characteristics of Low-Alcohol Kiwi Wine. *LWT* **2022**, *156*, 113049. [[CrossRef](#)]
35. Sereni, A.; Phan, Q.; Osborne, J.; Tomasino, E. Impact of the Timing and Temperature of Malolactic Fermentation on the Aroma Composition and Mouthfeel Properties of Chardonnay Wine. *Foods* **2020**, *9*, 802. [[CrossRef](#)]
36. Torrea, D.; Varela, C.; Ugliano, M.; Ancin-Azpilicueta, C.; Francis, I.L.; Henschke, P.A. Comparison of Inorganic and Organic Nitrogen Supplementation of Grape Juice—Effect on Volatile Composition and Aroma Profile of a Chardonnay Wine Fermented with *Saccharomyces Cerevisiae* Yeast. *Food Chem.* **2011**, *127*, 1072–1083. [[CrossRef](#)]
37. Hao, Y.; Li, J.; Zhao, Z.; Xu, W.; Wang, L.; Lin, X.; Hu, X.; Li, C. Flavor Characteristics of Shanlan Rice Wines Fermented for Different Time Based on HS-SPME-GC-MS-O, HS-GC-IMS, and Electronic Sensory Analyses. *Food Chem.* **2024**, *432*, 137150. [[CrossRef](#)] [[PubMed](#)]
38. Franceschi, D.; Lomolino, G.; Sato, R.; Vincenzi, S.; De Iseppi, A. Umami in Wine: Impact of Glutamate Concentration and Contact with Lees on the Sensory Profile of Italian White Wines. *Beverages* **2023**, *9*, 52. [[CrossRef](#)]
39. Gao, D.; Wang, C.; Shi, H.; Liang, H. Widely Targeted Metabonomic Analysis to Study Effect of GSH on Metabolites of Chardonnay Wine during Simulated Oxidation. *Fermentation* **2023**, *9*, 815. [[CrossRef](#)]
40. Liu, P.-T.; Yu, K.-J.; Li, Y.-T.; Duan, C.-Q.; Yan, G.-L. The Content of Linoleic Acid in Grape Must Influences the Aromatic Effect of Branched-Chain Amino Acids Addition on Red Wine. *Food Res. Int.* **2018**, *114*, 214–222. [[CrossRef](#)]
41. Hazelwood, L.A.; Daran, J.M.; Van Maris, A.J.A.; Pronk, J.T.; Dickinson, J.R. The Ehrlich Pathway for Fusel Alcohol Production: A Century of Research on *Saccharomyces Cerevisiae* Metabolism. *Appl. Environ. Microbiol.* **2008**, *74*, 2259–2266. [[CrossRef](#)] [[PubMed](#)]

**Disclaimer/Publisher’s Note:** The statements, opinions and data contained in all publications are solely those of the individual author(s) and contributor(s) and not of MDPI and/or the editor(s). MDPI and/or the editor(s) disclaim responsibility for any injury to people or property resulting from any ideas, methods, instructions or products referred to in the content.